

Control of Autophagy in *Chlamydomonas* Is Mediated through Redox-Dependent Inactivation of the ATG4 Protease¹

María Esther Pérez-Pérez*, Stéphane D. Lemaire, and José L. Crespo

Instituto de Bioquímica Vegetal y Fotosíntesis, Consejo Superior de Investigaciones Científicas-Universidad de Sevilla, Sevilla, Spain (M.E.P.-P., J.L.C.); and Sorbonne Universités, UPMC Univ Paris 06, CNRS, UMR8226, Laboratoire de Biologie Moléculaire et Cellulaire des Eucaryotes, Institut de Biologie Physico-Chimique, 75005 Paris, France (S.D.L.)

ORCID IDs: 0000-0003-0779-6665 (M.E.P.-P.); 0000-0003-3514-1025 (J.L.C.).

Autophagy is a major catabolic pathway by which eukaryotic cells deliver unnecessary or damaged cytoplasmic material to the vacuole for its degradation and recycling in order to maintain cellular homeostasis. Control of autophagy has been associated with the production of reactive oxygen species in several organisms, including plants and algae, but the precise regulatory molecular mechanisms remain unclear. Here, we show that the ATG4 protease, an essential protein for autophagosome biogenesis, plays a central role for the redox regulation of autophagy in the model green alga *Chlamydomonas reinhardtii*. Our results indicate that the activity of *C. reinhardtii* ATG4 is regulated by the formation of a single disulfide bond with a low redox potential that can be efficiently reduced by the NADPH/thioredoxin system. Moreover, we found that treatment of *C. reinhardtii* cells with norflurazon, an inhibitor of carotenoid biosynthesis that generates reactive oxygen species and triggers autophagy in this alga, promotes the oxidation and aggregation of ATG4. We propose that the activity of the ATG4 protease is finely regulated by the intracellular redox state, and it is inhibited under stress conditions to ensure lipidation of ATG8 and thus autophagy progression in *C. reinhardtii*.

Macroautophagy (hereafter termed autophagy) is a catabolic process by which eukaryotic cells degrade and recycle intracellular material, including proteins, membranes, ribosomes, and entire organelles, in response to stress or for proper differentiation and development. During autophagy, cytosolic components are engulfed in bulk within a double-membrane vesicle known as the autophagosome and delivered to the vacuole/lysosome for degradation to recycle needed nutrients or degrade toxic or damaged components (He and Klionsky, 2009; Mizushima et al., 2011; Liu and Bassham, 2012). Therefore, autophagy plays a fundamental role in cellular homeostasis and the response to stress. The degradation of intracellular components via autophagy can be selective or nonselective depending on the nature of cargo that is targeted to the vacuole, and several types of selective autophagy have been

reported such as mitophagy, pexophagy, or chlorophagy (Floyd et al., 2012; Schreiber and Peter, 2014; Oku and Sakai, 2016; Young and Bartel, 2016).

Autophagy is highly conserved through evolution. The autophagy process is mediated by autophagy-related (ATG) genes, which were originally identified in yeasts (Tsukada and Ohsumi, 1993) and subsequently in other eukaryotes, including animals, plants, and algae (Bassham et al., 2006; Díaz-Troya et al., 2008b; Avin-Wittenberg et al., 2012; Shemi et al., 2015). Among these ATG genes, a subgroup of around 18 genes is required for autophagosome formation and constitutes the autophagy core machinery in most eukaryotes. Core ATG proteins include the ATG8 and ATG12 ubiquitin-like conjugation systems that catalyze the covalent binding of the ubiquitin-like protein ATG8 to the phospholipid phosphatidylethanolamine (PE), an essential event in the formation of the autophagosome (Mizushima et al., 2011; Feng et al., 2014). The conjugation of ATG8 to PE is catalyzed by the sequential action of ATG4 (a Cys protease), ATG7 (E1-activating enzyme), ATG3 (E2-activating enzyme), and the ATG12-ATG5-ATG16 complex (E3-like ligase). First, the ATG4 protease cleaves nascent ATG8 at a conserved Gly residue located at the C terminus of the protein. Processed ATG8 is then activated by the E1-like enzyme ATG7, transferred to the E2-like enzyme ATG3, and finally conjugated to PE at the exposed Gly in a reaction that requires the participation of the E3-like ligase ATG12-ATG5-ATG16 (Mizushima et al., 2011; Feng et al., 2014). ATG8 is also recycled from

¹ This work was supported in part by Ministerio de Economía y Competitividad grants BFU2012-35913 and BFU2015-68216-P and Junta de Andalucía CVI-7336 (to J.L.C.), and Agencie Nationale de la Recherche grants 12-BSV5-0019 REDPRO2 and LABEX DYNAMO ANR-11-LABX-0011 (to S.D.L.).

* Address correspondence to eperez@ibvf.csic.es.

The author responsible for distribution of materials integral to the findings presented in this article in accordance with the policy described in the Instructions for Authors (www.plantphysiol.org) is: María Esther Pérez-Pérez (eperez@ibvf.csic.es).

M.E.P.-P., S.D.L., and J.L.C. designed research, analyzed data, and wrote the manuscript; M.E.P.-P. performed the experiments.

www.plantphysiol.org/cgi/doi/10.1104/pp.16.01582

the autophagosome membrane by the delipidating activity of ATG4 that cleaves the amide bond between ATG8 and PE (Kirisako et al., 2000). Hence, ATG4 can act both as a conjugating and deconjugating enzyme, and the fine regulation of these two activities is essential for the normal function of autophagy (Nair et al., 2012; Nakatogawa et al., 2012; Yu et al., 2012).

The autophagy machinery is well conserved in the plant kingdom, although some differences have been reported between plants and algae. Higher plants such as *Arabidopsis* (*Arabidopsis thaliana*), maize (*Zea mays*), or rice (*Oryza sativa*) evolved either small or large families for many of the core ATG genes (Bassham et al., 2006; Chung et al., 2009; Avin-Wittenberg et al., 2012) likely allowing specialized functions. However, all predicted ATG genes appear to be in single copy in the genome of several algal species, including the model green alga *Chlamydomonas reinhardtii* (Díaz-Troya et al., 2008b; Avin-Wittenberg et al., 2012; Pérez-Pérez and Crespo, 2014; Shemi et al., 2015). The availability of plant mutant collections and established techniques for gene silencing has been fundamental to understand the role of autophagy in the plant response to stress. The analysis of *Arabidopsis* mutants defective in core autophagy genes such as *ATG3*, *ATG4*, *ATG5*, *ATG7*, or *ATG10* revealed that autophagy plays a central role in the plant response to nutrient (nitrogen or carbon) starvation, different abiotic stresses, and pathogen infection (Li and Vierstra, 2012; Liu and Bassham, 2012; Avila-Ospina et al., 2014; Minina et al., 2014; Michaeli et al., 2016). Moreover, this catabolic process has been involved in the selective degradation of chloroplasts and peroxisomes in plants (Ishida et al., 2008; Farmer et al., 2013; Kim et al., 2013; Shibata et al., 2013). In algae, it has been reported that autophagy is activated in response to nitrogen or carbon limitation, oxidative stress, metal toxicity, endoplasmic reticulum (ER) stress, or virus infection (Pérez-Pérez et al., 2010, 2012; Davey et al., 2014; Goodenough et al., 2014; Pérez-Martin et al., 2014, 2015; Schatz et al., 2014).

Control of autophagy has been associated with the production of reactive oxygen species (ROS) in several systems. Upon starvation, human cells generate ROS, specifically H_2O_2 , that seem to be essential for autophagosome biogenesis and autophagic degradation (Scherz-Shouval et al., 2007). In the model yeast *Saccharomyces cerevisiae*, autophagy has also been linked with the cellular redox state. Incubation of yeast cells with the ROS inducer H_2O_2 triggers autophagy, whereas activation of autophagy by the TOR inhibitor rapamycin results in a pronounced increase of the total glutathione (reduced glutathione [GSH] + oxidized glutathione [GSSG]) pool, a marker of redox unbalance (Pérez-Pérez et al., 2014). In *Arabidopsis*, it has been demonstrated that oxidative damage caused by the ROS generators methyl viologen and H_2O_2 triggers autophagy, and accordingly plants defective in autophagy show enhanced sensitivity to oxidative stress (Xiong et al., 2007). In the same line, a strong correlation between the activation of autophagy and the accumulation of ROS in carotenoid-depleted cells or in response to methyl viologen or H_2O_2

treatment has been shown in *C. reinhardtii* (Pérez-Pérez et al., 2010; Perez-Perez et al., 2012).

Despite the extensive experimental evidence connecting autophagy and redox signaling, the precise molecular mechanisms by which ROS control this catabolic process are largely unknown. At present, ATG4 is the only ATG protein whose activity has been proposed to be redox regulated. The proteolytic activity of human ATG4A and ATG4B is reversibly inhibited by oxidation in a process that involves Cys-81, which may interfere with the activity of the nearby catalytic Cys-77 (Scherz-Shouval et al., 2007). The activity of the yeast ATG4 protease is also subject to redox regulation, although the underlying molecular mechanism differs from the one described in humans, because Cys-81 is not conserved in yeasts or other eukaryotes such as plants and algae (Pérez-Pérez et al., 2014). Indeed, we have recently demonstrated that yeast ATG4 is regulated by oxidoreduction of a single disulfide bond between Cys-338 and Cys-394. Mutation of any of these two cysteines resulted in loss of redox regulation of ATG4, and the mutant proteins displayed constitutive activation (Pérez-Pérez et al., 2014). Moreover, the small oxidoreductase thioredoxin (Trx) was identified in this study as a regulator of ATG4 activity based on its ability to efficiently reduce the regulatory disulfide bond in this protease (Pérez-Pérez et al., 2014). In plants, it has been shown that the activity of *Arabidopsis* ATG4a and ATG4b is reversibly inhibited by oxidation (Woo et al., 2014), although the underlying molecular mechanism has not been reported.

In this study, we unraveled the molecular mechanism that mediates the redox regulation of *C. reinhardtii* ATG4. This regulation controls oxidative inactivation of ATG4 under conditions that promote autophagy in *C. reinhardtii*.

RESULTS

Identification of ATG4 in *C. reinhardtii*

We have previously reported that a single ATG4 gene is conserved in the nuclear genome of *C. reinhardtii* and that an ATG8-proteolytic activity can be detected in total extracts from *C. reinhardtii* (Pérez-Pérez et al., 2010). According to the most up-to-date annotated version of the *C. reinhardtii* genome at the Joint Genome Institute (gene model version 5.5 at the Phytozome 10.3 database), the *C. reinhardtii* ATG4 gene (Cre12.g510100.t1.1) codes for a protein of 640 amino acids that contains two peptidase domains highly conserved among ATG4 proteins (Sugawara et al., 2005; Fig. 1A). The predicted size of *C. reinhardtii* ATG4 (approximately 65 kD) is significantly higher compared to ATG4 proteins from other organisms, including algae, plants, yeasts, or mammals. Amino acid sequence comparison of ATG4 proteins revealed a low identity in this family of proteases, with *Volvox carteri* being the closest ortholog to *C. reinhardtii* ATG4 (Supplemental Fig. S1). Phylogenetic analysis of ATG4 proteins also showed that ATG4 homologs comprise three main branches: fungi, metazoans, and the green

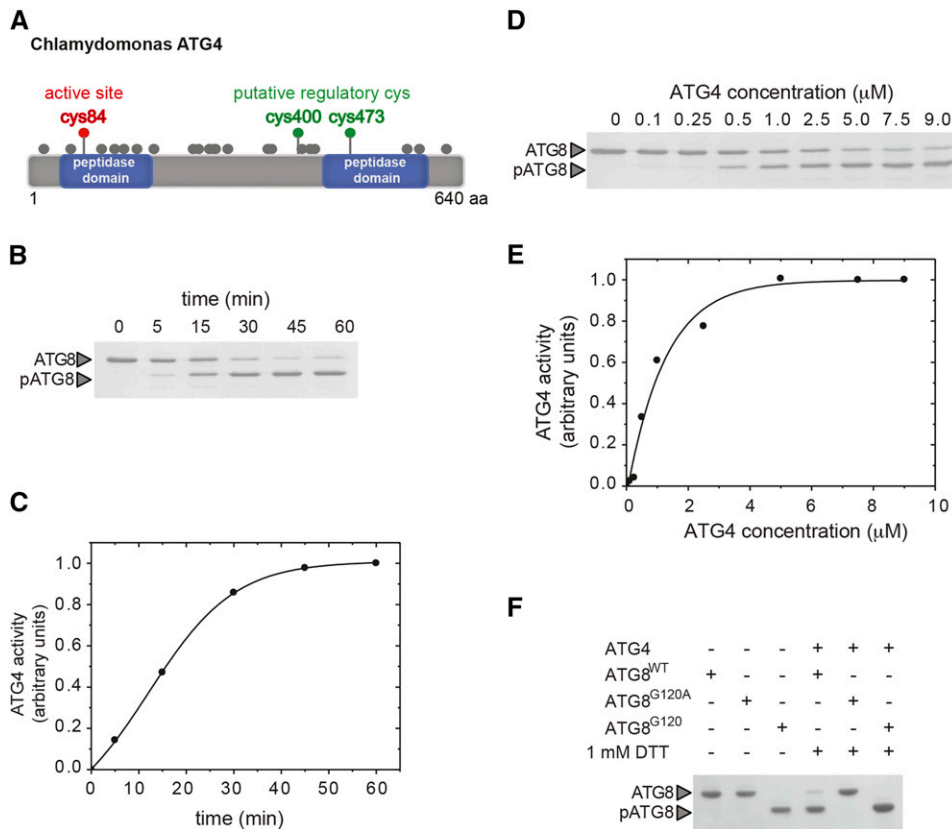


Figure 1. *C. reinhardtii* ATG4 cleaves ATG8 at the conserved Gly Gly-120. A, Domain structure of the ATG4 protease from *C. reinhardtii*. Two peptidase domains comprising residues from positions 49-182 and 437-590, respectively, were identified using the Conserved Domains search tool at the NCBI (<http://www.ncbi.nlm.nih.gov/Structure/cdd/wrpsb.cgi>). All cysteines present in *C. reinhardtii* ATG4 are indicated as gray balls, including the catalytic (red) and two putative regulatory (green) cysteines. B, *C. reinhardtii* ATG4 ($1 \mu\text{M}$) activity was monitored by following the cleavage of recombinant *C. reinhardtii* ATG8 ($5 \mu\text{M}$) from the unprocessed (ATG8) to the processed (pATG8) form (indicated by arrowheads) along time and subsequent SDS-PAGE and Coomassie Brilliant Blue staining. C, Quantification of ATG4 activity from B. The reference sample for quantification was the one at 60 min and it was considered as activity = 1 (in arbitrary units). D, Different concentrations of ATG4 were used to analyze C-terminal processing of ATG8 ($5 \mu\text{M}$) to pATG8 after 30 min. E, Quantification of ATG4 activity from D. The reference sample for quantification was the one with the maximum ATG4 concentration ($9 \mu\text{M}$) was considered as activity = 1, in arbitrary units). F, *C. reinhardtii* wild-type ATG8 (ATG8^{WT}) and the mutant forms ATG8^{G120A} (Gly-120 is replaced by Ala) and ATG8^{G120} (a truncated protein at Gly-120 corresponding to a processed-like form and used as a control) were incubated in an assay mixture in the absence or presence of the ATG4 protease for 1 h.

lineage, which includes green algae in a separate clade from land plants (Supplemental Fig. S2).

To characterize the ATG4 protein from *C. reinhardtii*, an in vitro assay was established using recombinant purified ATG4 and the ATG8 protein from *C. reinhardtii* as substrate. The endoproteolytic activity of ATG4 can be monitored by SDS-PAGE based on the different mobility of processed and unprocessed ATG8, since *C. reinhardtii* ATG8 contains a 15-amino acid extension at the C terminus of the protein that is cleaved by ATG4 (Kirisako et al., 2000; Pérez-Pérez et al., 2010). Our results indicated that ATG4 efficiently processes the C terminus of ATG8 within 15 to 30 min using a low concentration of the protease in the assay ($1 \mu\text{M}$; Fig. 1, B–E). To confirm that ATG8 processing occurs at the highly conserved Gly residue that is recognized by ATG4 (Kirisako et al., 2000), we performed a proteolytic assay with a mutant

version of ATG8 where Gly-120 has been replaced by Ala (ATG8^{G120A}) or a truncated form lacking the last 15 amino acids (ATG8^{G120}). As predicted, *C. reinhardtii* ATG4 cleaves ATG8 at the conserved Gly-120 (Fig. 1F).

C. reinhardtii ATG4 Activity Is Redox Regulated and Depends on a Single Disulfide Bond with a Very Low Redox Potential

It has been shown that the proteolytic activity of human and yeast ATG4 proteins is regulated by the reduction of a regulatory Cys adjacent to the catalytic Cys or the formation of a disulfide bond, respectively (Scherz-Shouval et al., 2007; Pérez-Pérez et al., 2014). To investigate whether the activity of *C. reinhardtii* ATG4 is subject to redox regulation, we performed an in-depth analysis of this protein under different redox conditions.

First, ATG4 was incubated with increasing concentrations of reducing (dithiothreitol [DTT]) or oxidant (H_2O_2) agents and processing of ATG8 was analyzed. ATG4 activity was enhanced with increasing concentrations of DTT (Fig. 2, A and B), indicating that the protein is activated by reduction. By contrast, the activity of ATG4 pre-reduced with a low concentration of DTT ($100 \mu\text{M}$) was inhibited by H_2O_2 in a concentration-dependent manner (Fig. 2, C and D). Moreover, we found that both reduction and oxidation of *C. reinhardtii* ATG4 are fully reversible (Fig. 2E), strongly suggesting that the regulation of ATG4 activity is controlled by redox posttranslational modifications. ATG4 proteins are Cys proteases whose activity is strictly dependent on a catalytic Cys that can be irreversibly blocked by alkylating agents such as iodoacetamide (IAM). *C. reinhardtii* ATG4 previously reduced and activated with low DTT was irreversibly inactivated by IAM, demonstrating that this protein is a Cys protease (Fig. 2F). Next, to determine if *C. reinhardtii* ATG4 activity depends on the redox potential, we analyzed ATG8 processing in the presence of different ratios of reduced and oxidized DTT (DTT_{red} and DTT_{ox} respectively; Fig. 2G). It was found that ATG4 is activated at a $\text{DTT}_{\text{red}}/\text{DTT}_{\text{ox}}$ ratio between 10^{-1} and 10^{-2} , suggesting that ATG4 activation requires a very low redox potential. In addition, we observed that *C. reinhardtii* ATG4 is activated by reduction with 1 mM DTT ($E_{m,7} = -330 \text{ mV}$) but not with GSH ($E_{m,7} = -240 \text{ mV}$) even at 5 mM (Fig. 2H), indicating again that a very low redox potential is required for ATG4 activation ($E_{m,7}$: midpoint redox potential at pH 7.0). Finally, we performed a complete DTT redox titration by varying the ambient redox potential (E_h at pH 7.0) between -232 and -350 mV . ATG4 was incubated at each potential, and the range of ATG4 activation was determined with the ATG8 processing assay (Fig. 2I). Our data indicated that there is a strong correlation between ATG4 activation and the redox potential. No significant activity was detected when the E_h was higher than -262 mV . The experimental data of this in-gel redox titration gave good fits to the Nernst equation for the reduction of a single 2-electron component, with a midpoint redox potential (E_m), at pH 7.0, of -278 mV (Fig. 2J). Thus, taken together, our data indicated that *C. reinhardtii* ATG4 activity is redox regulated and that the molecular mechanism of this redox regulation involves the oxidation of a single regulatory disulfide bond with a very low midpoint redox potential.

The NADPH/NTR/Trx System Regulates *C. reinhardtii* ATG4 Activity

Trx are small oxidoreductases that are able to reduce disulfide bonds with very low redox potentials (Buchanan and Balmer, 2005). To reduce a disulfide bond in a target protein, Trx has to be reduced first by the NADPH-dependent thioredoxin reductase (NTR), which takes electrons from NADPH (Jacquot et al., 1994). Trx can also receive electrons from DTT, a classical electron

donor widely used in biochemical assays to test the ability of Trx to reduce a target protein, since DTT is able to efficiently reduce Trx in vitro but reacts very slowly with the disulfide bond of the target protein. To test the ability of Trx to reduce and activate *C. reinhardtii* ATG4, TRXh1 from *C. reinhardtii*, the major cytosolic Trx (Lemaire and Miginiac-Maslow, 2004), was used in the ATG8 proteolytic assay. Our results indicated that TRXh1 efficiently activated the proteolytic activity of ATG4 in the presence of $10 \mu\text{M}$ DTT, whereas no ATG8 processing was detected in the presence of DTT only or when TRXh1 was replaced by a mutant form of this protein where the catalytic Cys is replaced by Ser (TRXh1^{C39S}; Fig. 3A). To further characterize the role of Trx in ATG4 reduction, we analyzed the time-course of ATG8 cleavage in the presence of TRXh1 and a very low concentration of DTT ($10 \mu\text{M}$). ATG4 was efficiently reduced and activated by TRXh1 but not with DTT alone or in the presence of TRXh1^{C39S} (Fig. 3B). Nevertheless, the physiological electron donor to TRXh1 is NTR rather than DTT, and therefore to investigate the regulation of *C. reinhardtii* ATG4 by TRXh1 we reconstituted the complete NADPH/NTR/Trx system using NTRB from Arabidopsis as electron donor for TRXh1. We observed that in the presence of the complete system, ATG4 is able to efficiently process ATG8, whereas no cleavage occurred when the reducing system was not complete or the mutant TRXh1^{C39S} was used (Fig. 3C). Therefore, our results strongly suggest a role of the NADPH/NTR/Trx system in the regulation of *C. reinhardtii* ATG4 by the oxidation of a regulatory disulfide bond.

Cys-400 Plays a Key Role in the Redox Control of *C. reinhardtii* ATG4

All our results indicate that a single disulfide bond may play a key role for the redox regulation of *C. reinhardtii* ATG4, as recently described for yeast ATG4 (Pérez-Pérez et al., 2014). Cys-338 and Cys-394 have been shown to establish a regulatory disulfide bond in yeast ATG4, and mutation of any of these residues results in constitutive activation of the protein (Pérez-Pérez et al., 2014). Cys-338 is widely conserved among ATG4 proteins, whereas Cys-394 seems to be restricted to some ascomycete species (Pérez-Pérez et al., 2014). Multiple sequence alignments revealed that the two regulatory cysteines identified in yeast ATG4 might be conserved in *C. reinhardtii* as Cys-400 and Cys-473, respectively (Supplemental Fig. S3). To test this hypothesis, Cys-400 and Cys-473 from *C. reinhardtii* ATG4 were mutated to Ser, and the corresponding recombinant proteins were produced and purified. We also identified Cys-84 as the catalytic Cys of *C. reinhardtii* ATG4. This Cys is the only one strictly conserved in all organisms (Supplemental Fig. S3). As expected, a mutant having this Cys replaced by Ser was constitutively inactive and was used as a negative control in these

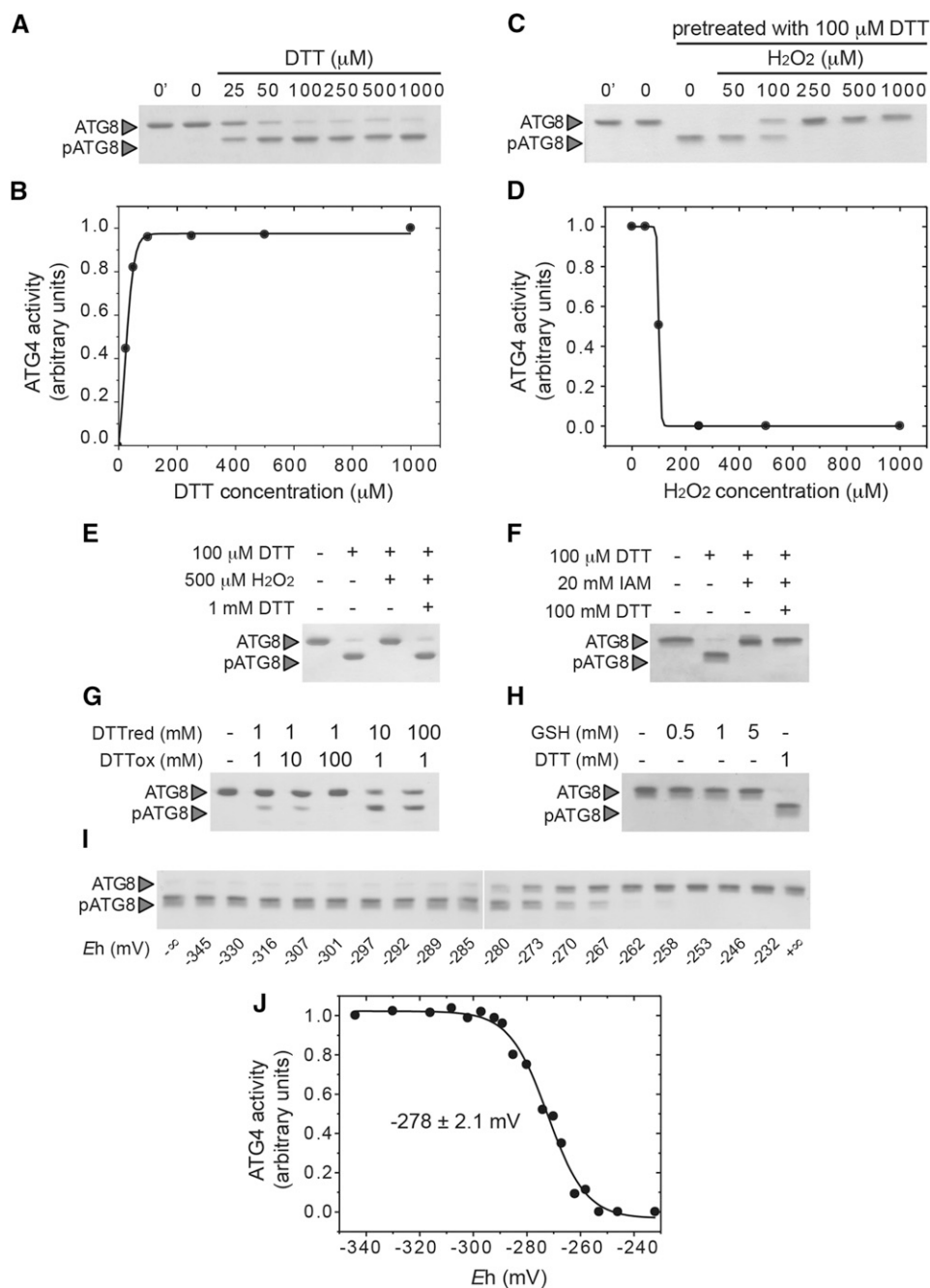


Figure 2. The protease activity of *C. reinhardtii* ATG4 is redox regulated. **A**, Effect of DTT on ATG4 activity. ATG4 was incubated with ATG8 for 1 h in the presence of DTT concentrations ranging from 25 μM to 1 mM. Control (lanes 1 and 2): incubation with no addition. Lane 1 does not contain ATG4. **B**, Quantification of ATG4 activity from **A**. The highest DTT concentration sample was used as reference sample for quantification (activity = 1, in arbitrary units). **C**, Effect of H₂O₂ on the activity of pre-reduced ATG4. After pretreatment with 100 μM DTT for 30 min, ATG4 was treated with increasing H₂O₂ concentrations for 20 min and then incubated with ATG8 for 1 h. Control (lanes 1 and 2): incubation with no addition. Lane 1 does not contain ATG4. **D**, Quantification of ATG4 activity from **C**. The pre-reduced but not treated with H₂O₂ sample was used as reference for quantification (activity = 1, in arbitrary units). **E**, Inhibition of ATG4 activity by H₂O₂ is reversed by DTT. ATG4 protein was pretreated with 100 μM DTT for 30 min (lane 2); then, ATG4 was incubated with 500 μM H₂O₂ for 20 min (lane 3); finally, ATG4 was newly treated with 1 mM DTT for 30 min (lane 4). Control (lane 1): incubation with no addition. For all lanes, ATG8 was added to the reaction mixture for 1 h after each specific treatment to assess ATG4 activity. **F**, ATG4 is irreversibly inactivated by the alkylating agent IAM. ATG4 was pretreated with 100 μM DTT for 30 min (lane 2), then incubated with 20 mM IAM for 30 min (lane 3); next, ATG4 was again incubated with 50 mM DTT for 30 min (lane 4). Control (lane 1): incubation with no addition. For all lanes, ATG8 was added to the reaction mixture for 1 h after each specific treatment to study ATG4 activity. **G**, ATG4 activity is

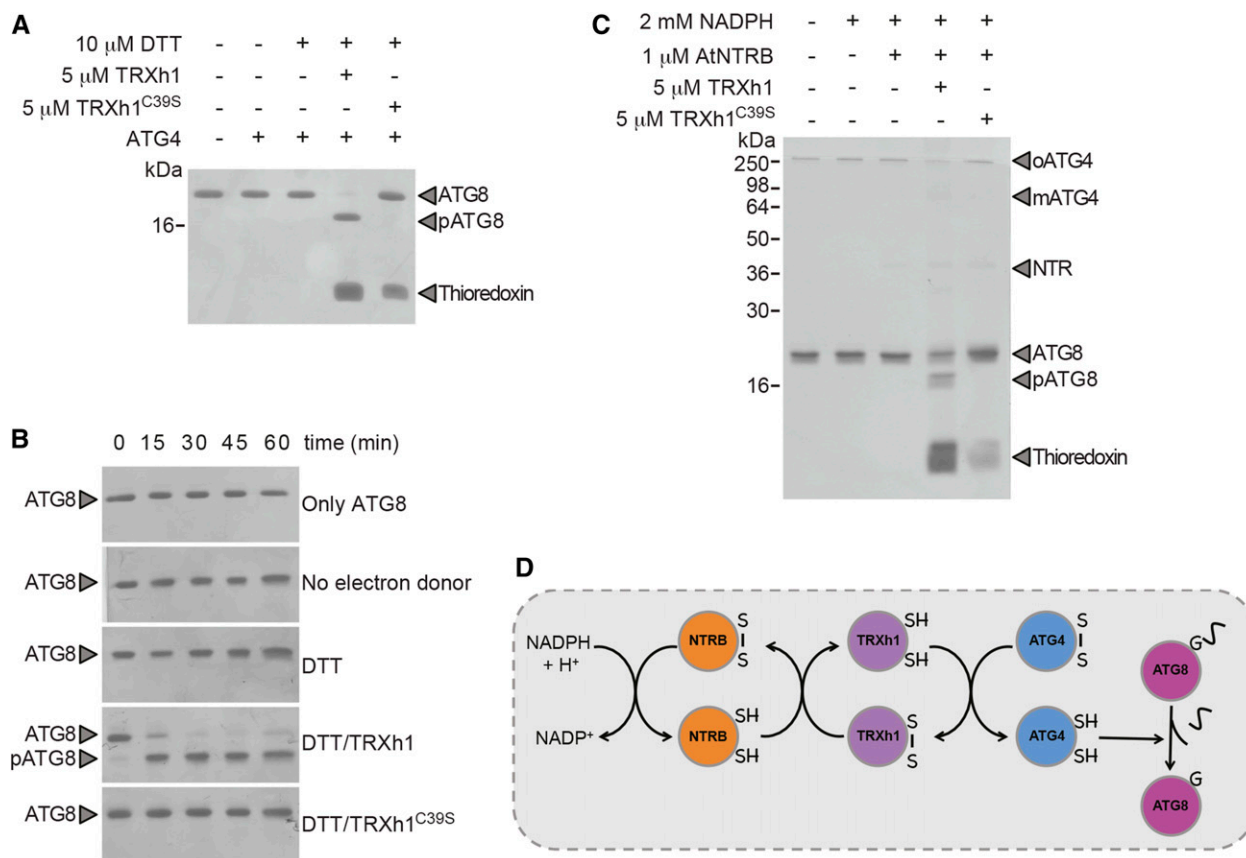


Figure 3. *C. reinhardtii* ATG4 is activated by the NADPH/NTR/TRX system. A, ATG4 activity was measured after incubation for 30 min in the presence (+) or absence (–) of 10 μ M DTT, 5 μ M TRXh1, and 5 μ M TRXh1^{C39S} as indicated. Proteins were visualized by Coomassie Brilliant Blue staining. pATG8, processed ATG8. B, Kinetics of ATG8 processing by ATG4 in the presence of 10 μ M DTT, 5 μ M TRXh1, or 5 μ M TRXh1^{C39S}. ATG4 activity was assayed as described in A. C, ATG4 activity was determined as described in (A) but using NADPH and NTR as the physiological electron donor for TRX. ATG4 activity was analyzed after incubation for 30 min in the presence (+) or absence (–) of 2 mM NADPH, 1 μ M Arabidopsis NTRB, 5 μ M TRXh1, and 5 μ M TRXh1^{C39S} as indicated. The ATG8 and pATG8 forms NTRB and TRXh1 are marked with arrowheads. D, Schematic representation of the proposed mechanism of activation of *C. reinhardtii* ATG4 through reduction by the NADPH/NTR/Trx system.

experiments (Fig. 4). The ATG8 cleavage activity of all ATG4 variants was analyzed in the presence of a low concentration of DTT with or without TRXh1. As mentioned above, wild-type ATG4 was activated by reduction with TRXh1 but not by low DTT. As expected, the mutant lacking the catalytic Cys (ATG4^{C84S}) was inactive in all tested conditions (Fig. 4). In contrast, the ATG4^{C400S} mutant was readily active even in the

absence of TRXh1 (Fig. 4), indicating that Cys-400 is required for the redox control of *C. reinhardtii* ATG4. However, mutation of Cys-473 had no effect on the proteolytic activity of the protein, strongly suggesting that this Cys does not participate in the redox regulation of *C. reinhardtii* ATG4 (Fig. 4). Nevertheless, the biochemical study performed on *C. reinhardtii* ATG4 demonstrated that the activity of this protein is regulated

Figure 2. (Continued.)

dependent on the DTT_{red}/DTT_{ox} ratio. ATG4 processing activity was monitored after incubation during 2 h in the presence of various DTT_{red}/DTT_{ox} ratios (1/1, 1/10, 1/100, 10/1, 100/1 in mM). H, ATG4 is not activated by GSH. ATG4 activity was determined after incubation for 1 h in the presence of 0.5, 1, or 5 mM GSH (lanes 2, 3, and 4, respectively), 1 mM DTT (lane 5), or in the absence of reducing agent (lane 1). I, Redox titration of ATG4 activity. ATG4 activity was analyzed after incubation for 2 h at indicated E_h poised by 20 mM DTT in various dithiol/disulfide ratios. ATG8 was added to the reaction mixture for 15 min after DTT treatment in all samples. The -∞ sample was used as reference for quantification. J, ATG4 activities monitored as in I were interpolated by nonlinear regression of the data using a Nernst equation for 2 electrons exchanged (n = 2) and one redox component. The average midpoint redox potential (E_{m,r}) of three independent experiments is reported in the figure as mean ± SD.

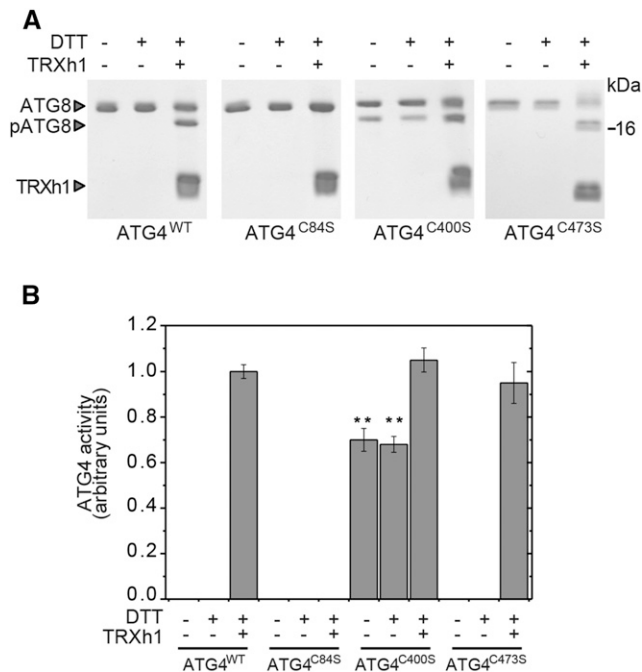


Figure 4. The Cys-to-Ser mutant protein ATG4^{C400S} is not redox-regulated. ATG4 activity was monitored as described in Figure 3. A, The activity of ATG4^{WT}, ATG4^{C84S}, ATG4^{C400S}, or ATG4^{C473S} was determined after incubation for 30 min in the presence (+) or absence (-) of 10 μ M DTT and 5 μ M TRXh1 as indicated. B, Quantification of ATG4 activity from A. The reference sample for quantification was ATG4^{WT} incubated with DTT and TRXh1 (activity = 1, in arbitrary units). The data are represented as mean \pm SD ($n = 3$). **, Differences were significant at $P < 0.01$ according to the Student's t test between the ATG4^{WT} and the indicated mutant. The ATG8 and pATG8 forms and TRXh1 are marked with arrowheads.

through the formation of a disulfide bond efficiently reduced by thioredoxin, where Cys-400 plays an important role.

Oligomerization of *C. reinhardtii* ATG4

In the course of the biochemical analysis of *C. reinhardtii* ATG4, we observed that this protein is able to oligomerize in the absence of 2-mercaptoethanol, an efficient reducer of disulfide bonds (Fig. 5A). Moreover, we found that the oligomerization of ATG4 is also redox regulated, since incubation of this protein with increasing DTT concentrations resulted in the monomerization of ATG4 (Fig. 5B), indicating that DTT prevents the aggregation of ATG4. However, treatment of ATG4 with H₂O₂ strongly stimulated the oligomerization of the protein in a reversible manner (Fig. 5, B and C). To further characterize the oligomerization of *C. reinhardtii* ATG4, we performed a DTT redox titration by incubating the protein with different concentrations of oxidized and reduced DTT. Our results revealed that there is a strong correlation between the oligomerization of *C. reinhardtii* ATG4 and the redox potential (Fig. 5D). Next, we investigated whether the

oligomerization of *C. reinhardtii* ATG4 might be conserved in other ATG4 proteins. We recently demonstrated that the proteolytic activity of yeast ATG4 is also controlled by the redox potential (Pérez-Pérez et al., 2014), although the study of the aggregation of this protein was not addressed. A detailed analysis of yeast ATG4 revealed that, interestingly, this protein shows an oligomerization pattern similar to the one described in *C. reinhardtii* ATG4, including the redox control of this process (Supplemental Fig. S4). Thus, taken together, these findings indicate that the redox regulation of ATG4 proteins may also involve the formation of aggregates in vitro.

Stress Conditions Promote the Oxidation and Aggregation of ATG4 in *C. reinhardtii*

To study the regulation of ATG4 in *C. reinhardtii* cells, we used an antibody raised against the recombinant protein. This antibody was able to recognize low amounts of purified *C. reinhardtii* ATG4 (Fig. 6A). We also tested the ability of this antibody to detect ATG4 in total extracts from *C. reinhardtii* cells. A band with a size comparable to *C. reinhardtii* ATG4 was observed in total extracts, although additional bands of lower and higher sizes could also be detected (Supplemental Fig. S3). The bands of lower size may likely correspond to degradation products of ATG4, whereas those of higher size might be due to posttranslational modifications or aggregation of this protein in vivo as observed with purified ATG4. To explore this hypothesis, we analyzed if the *C. reinhardtii* ATG4 antibody is able to detect monomeric and oligomeric ATG4. Our results revealed that indeed the antibody reacted with both forms of purified ATG4 (Fig. 6A).

Next, we investigated whether the detection of oligomeric ATG4 in *C. reinhardtii* total extracts may be related with the function of this protein in vivo. To this aim, ATG4 was analyzed in *C. reinhardtii* cells subjected to different stress conditions that activate autophagy in this organism. First, ATG4 was examined in stationary phase cells, since autophagy is up-regulated when *C. reinhardtii* cells reach stationary growth (Pérez-Pérez et al., 2010). We found that the abundance of ATG4, in particular oligomeric forms, increased in stationary cells (Fig. 6B). As previously reported (Pérez-Pérez et al., 2010), lipidated ATG8 could also be detected in stationary cells (Fig. 6B). Second, we investigated the effect of tunicamycin on ATG4, since this drug triggers ER stress and autophagy in *C. reinhardtii* (Pérez-Pérez et al., 2010). Our results indicated that monomeric and oligomeric ATG4 forms increased in tunicamycin-treated cells (Fig. 6C). Third, autophagy was also induced in *C. reinhardtii* by treating cells with norflurazon, an inhibitor of the carotene biosynthesis pathway (Sandmann and Albrecht, 1990) that activates this degradative process in *C. reinhardtii* as a result of ROS production and photo-oxidative damage of the cell (Pérez-Pérez et al., 2012). ATG8 lipidation was

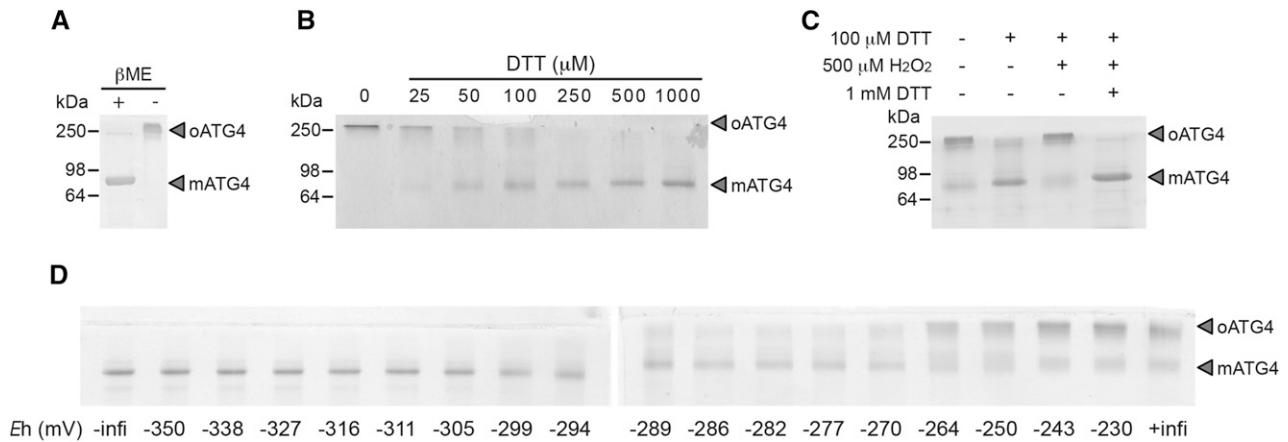


Figure 5. Redox control of *C. reinhardtii* ATG4 oligomerization. A, *C. reinhardtii* recombinant ATG4 (5 μM) was subjected to 12% SDS-PAGE in the presence (+) or absence (–) of β-mercaptoethanol (βME) and stained with Coomassie Brilliant Blue. mATG4, monomeric ATG4; oATG4, oligomeric ATG4. B, ATG4 (5 μM) was incubated with different DTT concentrations ranging from 25 to 1,000 μM for 1 h and then resolved by SDS-PAGE. C, ATG4 (5 μM) was preincubated with 100 μM DTT for 1 h (lane 2); then, ATG4 was treated with 500 μM H₂O₂ for 20 min (lane 3); and finally, ATG4 was incubated with 1 mM DTT for 30 min (lane 4). Control (lane 1): incubation with no addition. D, Redox titration of ATG4 oligomerization/monomerization. ATG4 monomerization was analyzed after incubation for 2 h at indicated E_h poised by 20 mM DTT in various dithiol/disulfide ratios. The oligomeric (oATG4) and monomeric (mATG4) ATG4 forms are marked by arrowheads. βME-free buffer was used in B to D.

detected in *C. reinhardtii* cells treated with norflurazon, as previously described (Pérez-Pérez et al., 2012; Fig. 6D). Monomeric and oligomeric forms of ATG4 were detected in cells with basal autophagy (Fig. 6D). However, activation of autophagy by norflurazon resulted in a pronounced detection of oligomeric ATG4 forms as well as an increase in the overall signal of ATG4 (Fig. 6D). Up-regulation of autophagy in stationary cells also increased the abundance of oligomeric ATG4 forms, although to a minor extent compared to cells treated with norflurazon for 48 h (Fig. 6D).

Finally, we also investigated the formation of ATG4 oligomers in the *C. reinhardtii* mutant *lts1-204*, which lacks phytoene synthase (McCarthy et al., 2004), one of the first enzymes in the carotenoid biosynthetic pathway. Carotenoid-less *lts1-204* cells grow in the dark on acetate-containing medium and are unable to survive in the light even under very low light conditions (McCarthy et al., 2004). We have previously shown that shifting *lts1-204* cells from dark to light results in a strong production of ROS and the activation of autophagy (Pérez-Pérez et al., 2012). Thus, we analyzed the effect of light on ATG4 abundance and oligomerization in the *lts1-204* mutant strain. In close agreement with the data obtained in norflurazon (NF)-treated cells, we found that both ATG4 abundance and oligomerization significantly increased in mutant cells exposed to light (Fig. 6E). As previously shown (Pérez-Pérez et al., 2012), ATG8 was also up-regulated in light-stressed *lts1-204* cells (Fig. 6E). Taken together, our results indicate that stress conditions that generate ROS and

activate autophagy promote the oxidation and aggregation of ATG4 in *C. reinhardtii*.

ATG4 Activity Depends on ATG4 Reduction and Monomerization

We reasoned that the oxidation and aggregation of ATG4 observed in *C. reinhardtii* cells treated with NF might be due to the high production of ROS that takes place in these cells (Pérez-Pérez et al., 2012). To explore this hypothesis, we treated *C. reinhardtii* cells with NF in the presence or absence of the ROS scavenger *N*-acetyl Cys (NAC). We observed that NAC largely prevented the effect of NF on ATG4 (Fig. 7A). Remarkably, the presence of NAC also decreased the lipidation of ATG8 in cells treated with NF (Fig. 7A), again supporting the role of ROS in the activation of autophagy in these cells (Pérez-Pérez et al., 2012) through inhibition of ATG4.

To further investigate the formation of oligomeric ATG4, total extracts from stationary cells were incubated with DTT, and the aggregation of ATG4 was analyzed by western blot. Our results revealed that oligomeric ATG4 was converted into monomeric ATG4 by reduction with DTT and demonstrated that oligomerization of ATG4 is redox regulated in *C. reinhardtii* (Fig. 7B, top panel). Next, we investigated whether aggregated ATG4 may represent an inactive state of the protein. To this aim, we assayed the ATG4 proteolytic activity present in total extracts from *C. reinhardtii* cells using recombinant 6His-ATG8 as substrate as previously described (Pérez-Pérez et al., 2010). Our results indicated that DTT stimulated the proteolytic activity of

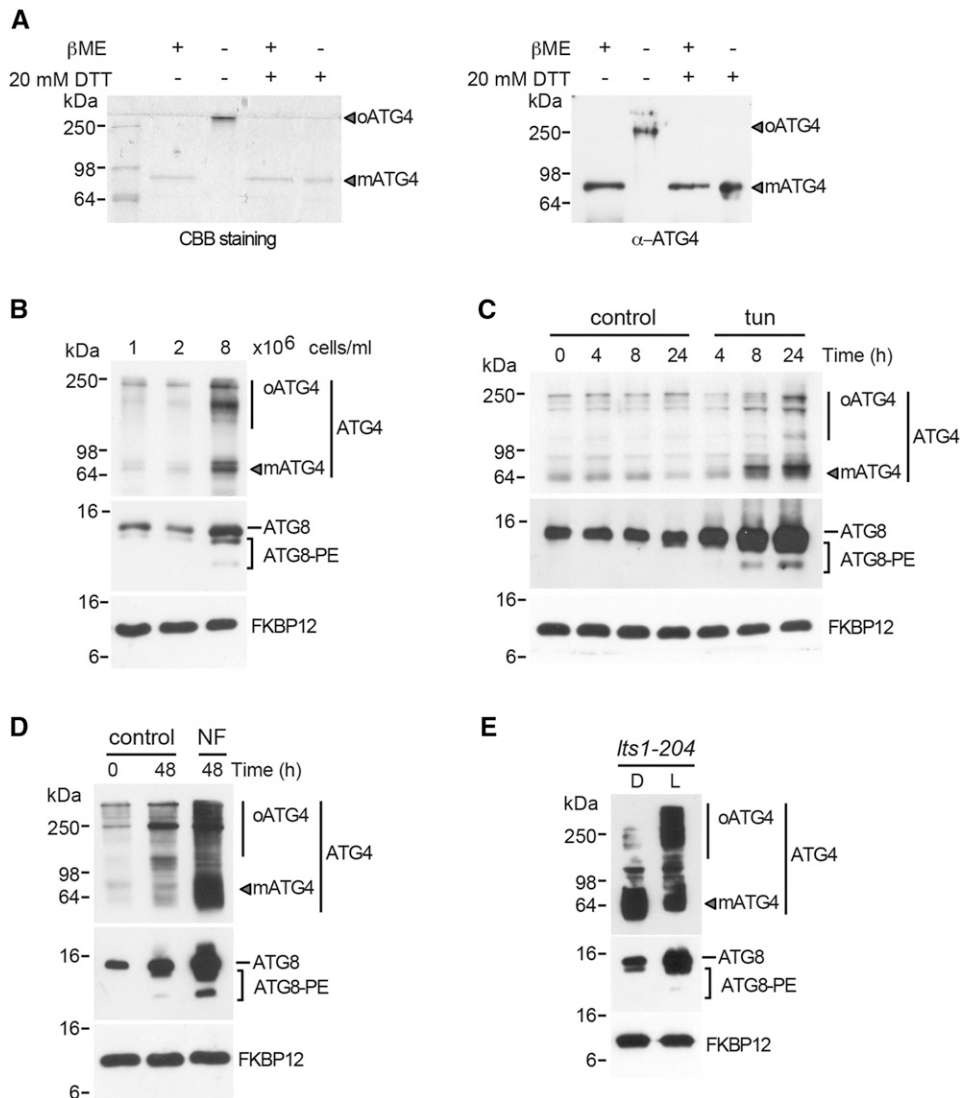


Figure 6. Autophagy-activating conditions lead to the oligomerization and inactivation of ATG4 in *C. reinhardtii* cells. **A**, *C. reinhardtii* recombinant ATG4 was subjected to 12% SDS-PAGE in the presence (+) or absence (–) of β -mercaptoethanol (β ME) in the loading buffer and/or treated with 20 mM DTT for 1 h and then stained with Coomassie Brilliant Blue (5 μ M ATG4) or subjected to western-blot analysis with anti-ATG4 antibodies (0.25 μ M ATG4). **B**, Western-blot analysis of ATG4 and ATG8 during the growth phase in *C. reinhardtii*. Cells were grown in TAP from 1×10^6 cells/mL to 8×10^6 cells/mL, and the ATG4 and ATG8 protein profiles were analyzed. **C**, Effect of ER stress on ATG4 and ATG8 in *C. reinhardtii*. Wild-type *C. reinhardtii* cells growing at exponential phase were treated with 5 μ g/mL tunicamycin (tun) as previously described (Pérez-Pérez et al., 2010), and samples were taken at different times for its analysis. Untreated cells were used as control. **D**, Inhibition of the carotenoid biosynthetic pathway leads to ATG8 lipidation and ATG4 oligomerization in *C. reinhardtii*. Wild-type *C. reinhardtii* cells in exponential growth phase were treated with 20 μ M NF during 48 h as previously described (Pérez-Pérez et al., 2012). Samples of nontreated cells were taken at the same time and used as control. **E**, Western-blot analysis of ATG4 and ATG8 proteins on dark-to-light transition in the *lts1-204* mutant. *C. reinhardtii lts1-204* cells growing exponentially in TAP under dark conditions were transferred to standard light illumination (25 μ E) for 6 h. Cells maintained in dark conditions were used as control. Then 15 μ g of total extracts were resolved by 12% (for ATG4) or 15% (for ATG8 and FKBP12) SDS-PAGE followed by western blotting with anti-ATG4, anti-ATG8, and anti-FKBP12 antibodies. The oligomeric (oATG4) and monomeric (mATG4) ATG4 forms are marked on the right. Molecular mass markers (kD) are indicated on the left. β -Mercaptoethanol-free buffer was used in B to E.

ATG4 (Fig. 7B, bottom panel). Furthermore, we found that incubation with IAM resulted in ATG4 inactivation and had no effect on the conformation of the protein (Fig. 7, B and C), indicating that aggregated,

oxidized ATG4 is inactive. This finding was also confirmed in vitro using purified ATG4 and ATG8 proteins. DTT efficiently reduced and activated recombinant ATG4, and a tight correlation between

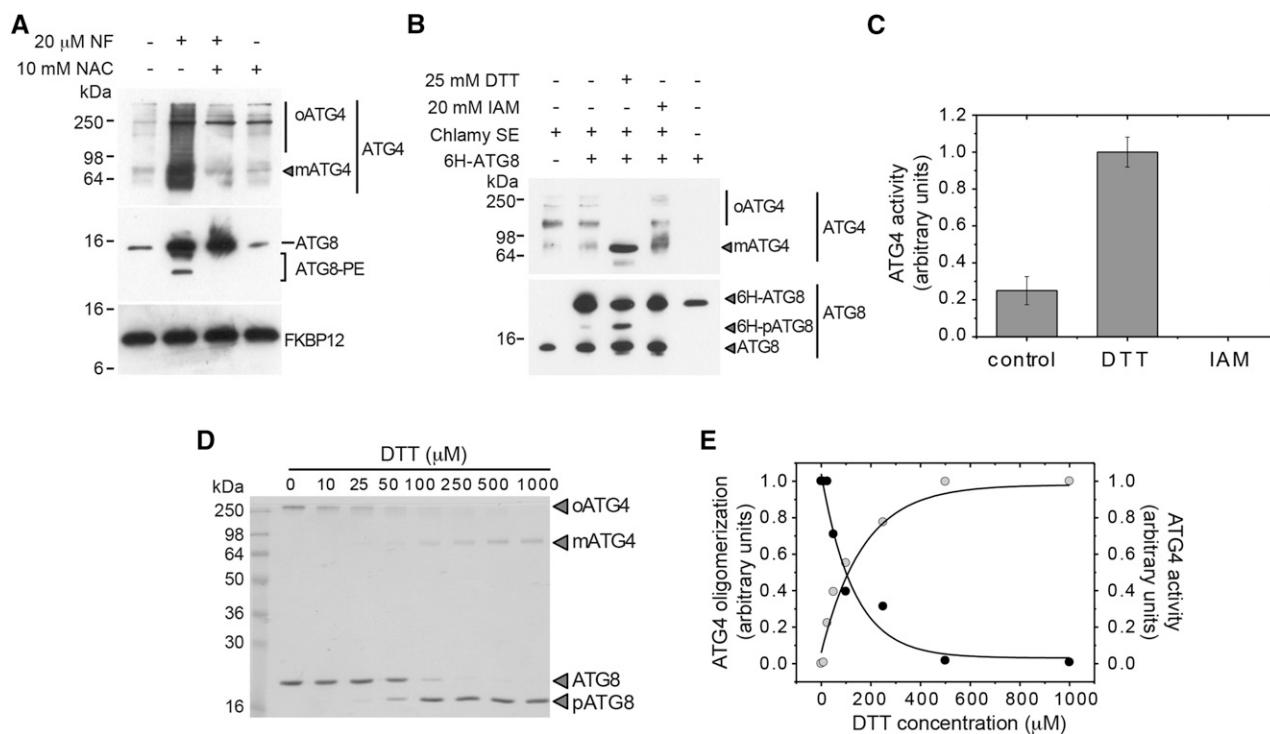


Figure 7. ATG4 activity depends on ATG4 reduction and monomerization. A, The ROS scavenger NAC decreased ATG4 oxidation and aggregation in *C. reinhardtii*. Wild-type *C. reinhardtii* cells in exponential growth phase were treated with 20 μ M NF in the presence (+) or absence (–) of 10 mM NAC during 48 h. Samples of nontreated cells were taken before the treatment(s) and used as control (first lane). B, ATG4 protease activity in cell-free extracts of *C. reinhardtii*. Ten nanograms of recombinant His-tagged ATG8 protein (6H-ATG8) were incubated with 50 μ g of cell-free extracts of *C. reinhardtii* for 30 min at 25°C. When required, cell-free extracts were previously incubated with a reducing (25 mM DTT) or alkylating (20 mM IAM) agent for 1 h on ice. The reaction was stopped by the addition of loading buffer and boiling at 100°C. Aliquots of the reaction mixtures were resolved by 15% SDS-PAGE and analyzed by western blotting with the anti-ATG4 (top panel) and anti-ATG8 (bottom panel) antibodies. Exogenous, recombinant ATG8 protein containing the His-6 tag (6H-ATG8) could be distinguished from endogenous *C. reinhardtii* ATG8 by their different size (Pérez-Pérez et al., 2010). The oligomeric (oATG4) and monomeric (mATG4) ATG4 forms, the unprocessed (6H-ATG8) and processed His-tagged (p6H-ATG8) ATG8 forms, and the endogenous ATG8 protein (ATG8) are marked with arrowheads. C, Quantification of ATG4 activity from B. Three independent experiments were used for quantification and they are shown as mean \pm SD. D, Effect of DTT on both ATG4 oligomerization and ATG4 activity. Purified ATG4 (2.5 μ M) was incubated with ATG8 (5 μ M) for 30 min in the presence of DTT concentrations ranging from 10 to 1 mM. Control (lane 1): incubation with no addition. The oligomeric (oATG4) and monomeric (mATG4) ATG4 forms, and the unprocessed (ATG8) and processed ATG8 (pATG8) forms are marked by arrowheads. Molecular mass markers (kD) are shown on the left. A β -mercaptoethanol-free buffer was used. E, Quantification of ATG4 oligomerization (black circles) and ATG4 activity (dark-gray circles) from D. The DTT-lacking sample and the highest DTT concentration-sample were used as reference sample for quantification of oligomerization (oligomerization = 1, in arbitrary units) and quantification of activity (activity = 1, in arbitrary units), respectively. Three independent experiments were used for quantification.

ATG4 reduction/monomerization and ATG8 processing was detected with increasing concentrations of DTT (Fig. 7, D and E).

Aggregated ATG4 Localizes to Punctate Structures in *C. reinhardtii* Cells

We analyzed the cellular localization of ATG4 by immunofluorescence microscopy in *C. reinhardtii* cells treated or not with NF. In control untreated cells, the ATG4 signal was weak and restricted to some spots localized to the apical end of the cell as revealed by basal body staining with an antiacetylated tubulin antibody (Díaz-Troya et al., 2008a; Fig. 8). Progression into stationary phase of

untreated cells resulted in a moderate increase of ATG4 signal and the detection of intense spots in other parts of the cell in addition to the peri-basal body region (Fig. 8). Remarkably, NF treatment caused a pronounced increase of ATG4 signal and more intense dots were readily observed (Fig. 8). Based on these results and the finding that ATG4 aggregates in response to NF treatment, the punctate structures observed in treated cells may likely contain aggregated ATG4. To strengthen this hypothesis, we also investigated the localization of ATG4 in *lts1-204* mutant cells shifted from dark to light, since this stress strongly promotes ATG4 oligomerization (Fig. 6E). In agreement with the punctate pattern observed in wild-type cells treated with NF (Fig. 8), light stress in carotenoid-mutant

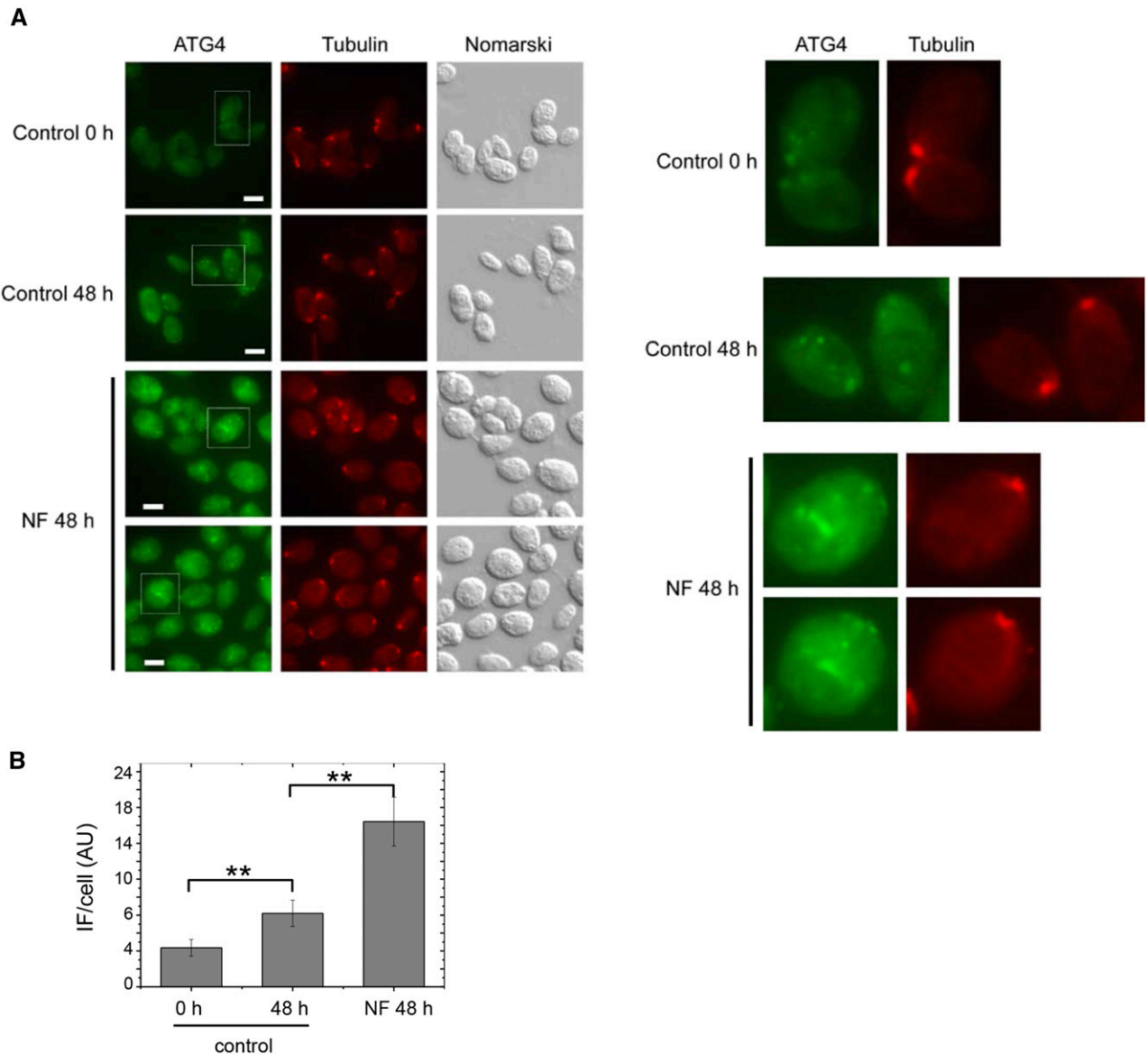


Figure 8. ATG4 localizes to punctate structures in *C. reinhardtii* cells in response to autophagy activation. A, Immunolocalization of ATG4 in wild-type *C. reinhardtii* cells treated with NF. *C. reinhardtii* cells growing exponentially were treated with 20 μM NF for 48 h. Nontreated cells at 0 and 48 h were used as control. Cells were collected and processed for immunofluorescence microscopy analysis with anti-ATG4 and antiacetylated tubulin antibodies. Scale bar = 8 μm . A zoom of some of the cells is also shown (right panels for the control cells and lower panels for NF-treated cells). B, Quantification of the immunofluorescence signal detected in individual cells from the experiment described in A. A minimum of 200 cells was analyzed for each condition using ImageJ software. ** Differences were significant at $P < 0.0001$ according to Student's *t* test. AU, arbitrary units.

cells resulted in a sharp localization of ATG4 in a central region of the cell (Fig. 9). Altogether, these results indicate that ROS-generating stress leads to the detection of ATG4 as intense spots likely containing oligomeric forms of this protein.

DISCUSSION

Recent genomic analyses revealed that core autophagy genes are highly conserved among plants and algae

(Díaz-Troya et al., 2008b; Avin-Wittenberg et al., 2012; Pérez-Pérez and Crespo, 2014; Shemi et al., 2015). However, our current knowledge about the molecular mechanisms that regulate most of the ATG proteins in the plant kingdom is limited compared to yeasts or mammals. In this study, we unraveled the molecular mechanism underlying the redox regulation of the ATG4 protease from the model green alga *C. reinhardtii*. A single *ATG4* gene has been previously identified in *C. reinhardtii* (Díaz-Troya et al., 2008b) as well as in other green algae (Pérez-Pérez and Crespo, 2014; Shemi et al.,

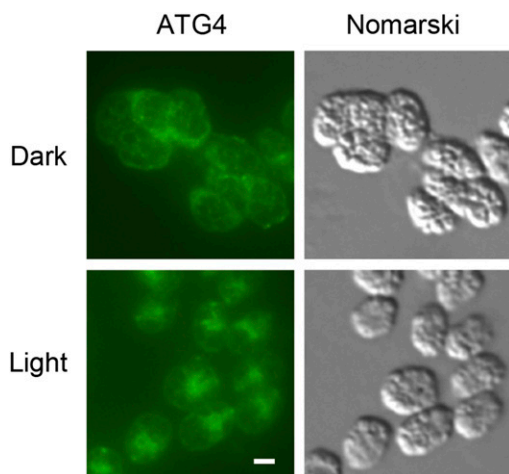


Figure 9. Localization of ATG4 in *C. reinhardtii* carotenoid mutant cells exposed to light. *Its1-204* mutant cells growing exponentially in TAP medium in dark conditions were exposed to low light ($20 \mu\text{E m}^{-2} \text{s}^{-1}$) for 6 h or maintained in dark conditions as control. Cells were collected and processed for immunofluorescence microscopy analysis with anti-ATG4 antibodies. Scale bar = $8 \mu\text{m}$.

2015), whereas plants such as *Arabidopsis*, maize, or rice have two *ATG4* genes (Yoshimoto et al., 2004; Chung et al., 2009; Avin-Wittenberg et al., 2012). Amino acid sequence comparison of ATG4 proteins from different organisms showed a low identity even in the green lineage (Supplemental Figs. S1 and S2). The ATG4 protein from *C. reinhardtii* is about 200 to 300 amino acids larger than its orthologs in yeasts, plants, or mammals, which might indicate that this protein has acquired additional domains in *C. reinhardtii*. In this regard, an unusually large (about 3,800 amino acids) ATG4 protein with ATG8-endoproteolytic activity has been reported in the parasitic protist *Toxoplasma gondii* (Kong-Hap et al., 2013). The low identity found among ATG4 proteases together with their variable size suggests that this key autophagy protein may have developed specific features and/or functions in evolutionarily distant eukaryotes.

Our results demonstrated that the activity of *C. reinhardtii* ATG4 is subjected to redox regulation, since the protein is active in the reduced form and inactive in the oxidized form. Moreover, we found that this regulation is reversible, suggesting the involvement of redox posttranslational modifications. A similar redox regulation has been reported for yeast, human, and *Arabidopsis* ATG4 (Scherz-Shouval et al., 2007; Pérez-Pérez et al., 2014; Woo et al., 2014), indicating that the redox control of ATG4 activity is broadly conserved in eukaryotes despite the low identity observed among ATG4 proteins. The mechanism of action by which redox signals control ATG4 activity has been shown in only mammals and yeasts. In human ATG4A and ATG4B, this redox regulation involves Cys-81, which interferes with the activity of the adjacent catalytic

Cys-77 (Scherz-Shouval et al., 2007). Regulatory Cys-81 from human ATG4s is not conserved in yeasts, and consequently the molecular mechanism that mediates the redox control of ATG4 in this unicellular model system is different. A detailed biochemical analysis demonstrated that Atg4 activity is controlled in yeasts through dithiol/disulfide exchange that involves the transfer of two electrons and the oxidation/reduction of a single disulfide bond (Pérez-Pérez et al., 2014). Our studies on the ATG4 protein from *C. reinhardtii* are in close agreement with these findings, since the redox characterization of this protein indicated that the activity of *C. reinhardtii* ATG4 is regulated by the reduction of a single disulfide bond with a very low redox potential. In the cell, these regulatory disulfides with very low redox potential are typically reduced by small oxidoreductases such as thioredoxins (Buchanan and Balmer, 2005). Indeed, it has been shown that yeast ATG4 can be efficiently reduced and activated by the cytoplasmic thioredoxin Trx1 (Pérez-Pérez et al., 2014). We found that *C. reinhardtii* ATG4 also can be readily reduced by the cytoplasmic thioredoxin TRXh1 from this alga, suggesting that control of ATG4 activity by thioredoxins might be evolutionarily conserved. In close agreement, thioredoxin and thioredoxin reductase have been identified as autophagosome-associated proteins in a quantitative proteomic study (Dengjel et al., 2012). Moreover, we were able to reconstitute in vitro the whole ATG4 redox regulation process by the NADPH/NTR/thioredoxin system using NTRB from *Arabidopsis* as electron donor for *C. reinhardtii* TRXh1. The finding that NADPH can act as the electron donor of *C. reinhardtii* ATG4 suggests that this reducing molecule may link the energetic and redox state of the cell with the regulation of the autophagy process through the control of ATG4 activity.

Site-directed mutagenesis established that the regulatory disulfide bond in yeast Atg4 is formed between Cys-338 and Cys-394 (Pérez-Pérez et al., 2014). Cys-338 appears to be conserved in yeasts, plants, and mammals, whereas Cys-394 is restricted to some ascomycete species (Pérez-Pérez et al., 2014). Our results demonstrated that Cys-400 (the equivalent to Cys-338 in yeast Atg4) is required for the redox regulation of *C. reinhardtii* ATG4 activity and strengthen the hypothesis that the key role of this residue in the control of ATG4 is conserved through evolution. However, we found that Cys-473 (the counterpart to Cys-394 in yeast Atg4) does not participate in the redox regulation of ATG4 activity, since point mutation of this residue had no significant effect on the redox control of this protein. This observation is consistent with the poor conservation of Cys-394 from yeast ATG4 in other organisms (Pérez-Pérez et al., 2014). Nevertheless, the finding that *C. reinhardtii* ATG4 activity is regulated through the reduction of a single disulfide bond by thioredoxin and that one of the regulatory cysteines is conserved strongly suggests that the mechanism of ATG4 regulation is evolutionarily conserved in unicellular eukaryotes like yeasts and algae.

We found that ATG4 is oxidized and forms oligomers in *C. reinhardtii* cells treated with NF, an inhibitor of the carotenoid biosynthesis pathway that generates high levels of ROS and activates autophagy in this green alga (Pérez-Pérez et al., 2012). ATG4 aggregates were also observed in the carotenoid-less mutant *lts1-204* exposed to light, a stress condition that produces ROS and induces autophagy (Pérez-Pérez et al., 2012), or when wild-type cells reached stationary growth, a physiological condition that triggers autophagy in *C. reinhardtii* (Pérez-Pérez et al., 2010). Concomitant with ATG4 aggregation, we also detected an accumulation of lipidated ATG8 under all these stress conditions, strongly suggesting that aggregated ATG4 is inactive. Together, our results provide the molecular basis for the redox control of autophagy in a photosynthetic organism through the oxidation and inactivation of the ATG4 protease under stress conditions.

MATERIALS AND METHODS

Strains, Media, and Growth Conditions

Chlamydomonas reinhardtii wild-type 4A+ (CC-4051) and the *lts1-204* mutant (CC-4199) strains were obtained from the *Chlamydomonas* Culture Collection. *C. reinhardtii* cells were grown under continuous illumination at 25°C in Tris-acetate phosphate (TAP) medium as described (Harris, 1989). When required, cells in exponential growth phase (10^6 cells/mL) were treated with NF (Sigma-Aldrich; 34364). The *lts1-204* mutant strain was maintained in complete darkness as previously described (McCarthy et al., 2004).

Gene Cloning and Protein Purification

The DNA coding sequence of the *ATG4* gene from *C. reinhardtii* was synthesized and cloned into pBluescript SK (+) vector by GeneCust Europe (<http://www.genecust.com>). The *ATG4* coding region was cloned into the pET28a (+) (Novagen; 69864-3) plasmid at *NdeI* and *XhoI* sites for expression of the corresponding His-tagged protein. The different *ATG4* mutants (*ATG4*^{C84S}, *ATG4*^{C400S}, and *ATG4*^{C473S}) were synthesized by GeneCust Europe and cloned into pBluescript SK (+) vector. The different *ATG4* mutants were also cloned into the pET28a (+) plasmid at *NdeI* and *XhoI* sites. All clones were verified by DNA sequencing and used to transform *Escherichia coli* BL21 (DE3) strain. Recombinant proteins were expressed by induction at exponential growth phase ($OD_{600} \approx 0.5$) with 0.5 mM isopropyl- β -D-thiogalactopyranoside (Sigma-Aldrich; I6758) for 2.5 h at 37°C. The recombinant proteins *ATG4*^{WT}, *ATG4*^{C84S}, *ATG4*^{C400S} and *ATG4*^{C473S} were purified by affinity chromatography on a His-Select Nickel Affinity Gel (Sigma-Aldrich; P6611) following the manufacturer's instructions. Prior to purification, wild-type ATG4 and the Cys variants were first solubilized with 4 M urea (Sigma-Aldrich; 51456) due to the presence of the recombinant proteins in inclusion bodies and subsequently purified from the soluble fraction by affinity chromatography as described above. The ATG8 protein from *C. reinhardtii* and the ATG4 protein from *Saccharomyces cerevisiae* were purified as previously described (Pérez-Pérez et al., 2010, 2014), respectively. The TRXh1^{WT} and TRXh1^{C395S} proteins from *C. reinhardtii* were purified as described in Goyer et al. (1999). The NTRB protein from *Arabidopsis thaliana* was purified as described in Jaquot et al. (1994). All proteins used in this study are listed in Supplemental Table S1.

In Vitro ATG4 Cleavage Assay

A typical reaction mixture included 1 μ M ATG4, 5 μ M ATG8, 1 mM 1,4-DTT (Sigma-Aldrich; 43815), and 1 mM EDTA (Sigma-Aldrich; E6511) in 50 mM Trizma base, 138 mM NaCl, and 27 mM KCl, pH 8. When indicated, ATG4 was preincubated in the presence of reducing [DTT (Sigma-Aldrich; 43815) or GSH (Sigma-Aldrich; G4251)], oxidizing [DTTox (Sigma-Aldrich; D3511) or H₂O₂ (Sigma-Aldrich; H1009)], or alkylating [IAM (Sigma-Aldrich; I1149)] compounds alone or in combination at the indicated times and concentrations. For the analysis

of TRX activity, 10 μ M DTT and 5 μ M TRXh1 or TRXh1^{C395S} from *C. reinhardtii* were used at the indicated incubation time. The reaction mixtures were incubated at 25°C for the indicated time and stopped by addition of β -mercaptoethanol-free Laemmli sample buffer followed by 5 min of boiling. Proteins were resolved on 15% SDS-PAGE gels and stained with Coomassie Brilliant Blue (Sigma-Aldrich; 27816). For ATG4 activity quantification, gels were scanned with Odyssey (LI-COR, Biosciences) and the signals corresponding to unprocessed (ATG8) and processed (pATG8) ATG8 were quantified with the software Image Studio (LI-COR, Biosciences). The ATG4 activity was considered as the relation between pATG8/(ATG8+pATG8), and it was normalized between 0 and 1, with 0 corresponding to totally oxidized and inactive ATG4 and 1 corresponding to totally reduced and active ATG4. The ATG4 activities (in arbitrary units) were plotted using the software OriginPro 8 (OriginLab).

Protein Preparation and Immunoblot Analysis

C. reinhardtii cells from liquid cultures were collected by centrifugation (4,000g for 5 min), washed in 50 mM Tris-HCl (pH 7.5) buffer, and resuspended in a minimal volume of the same solution. Cells were lysed by two cycles of slow freezing to -80°C followed by thawing at room temperature. The soluble cell extract was separated from the insoluble fraction by centrifugation (15,000g for 20 min) in a microcentrifuge at 4°C. For immunoblot analyses, total protein extracts (15 μ g) were subjected to 12% or 15% SDS-PAGE and then transferred to nitrocellulose membranes (Bio-Rad; 162-0115). Anti-CrATG4 (obtained in collaboration with Agrisera Antibodies), anti-CrATG8 (Pérez-Pérez et al., 2010), anti-CrFKBP12 (Crespo et al., 2005), and secondary antibodies were diluted 1:5,000, 1:3,000, 1:5,000, and 1:10,000, respectively, in PBS containing 0.1% (v/v) Tween 20 (Applichem; A4974) and 5% (w/v) milk powder. The Luminata Crescendo Millipore immunoblotting detection system (Millipore; WBLUR0500) was used to detect the proteins with horseradish peroxidase-conjugated antirabbit secondary antibodies (Sigma-Aldrich; A6154). Proteins were quantified with the Coomassie dye binding method (Bio-Rad; 500-0006).

In Vivo ATG4 Cleavage Assays

A typical reaction mixture contained 50 μ g total extract from *C. reinhardtii* and 10 ng of 6His-tagged ATG8 (denoted as 6H-ATG8). When indicated, reducing agent (25 μ M DTT) or alkylating agent (20 μ M IAM) was added. The reaction mixture was incubated at 25°C for the indicated time and stopped by addition of β -mercaptoethanol-free Laemmli sample buffer followed by 5 min of boiling. The samples were analyzed by western-blot analysis with anti-CrATG8 or anti-CrATG4 antibodies as described above.

Immunofluorescence Microscopy

C. reinhardtii-untreated (control 0 h and control 48 h) or NF-treated (NF 48 h) cells were fixed and stained for immunofluorescence microscopy as previously described (Crespo et al., 2005). The primary antibodies used were anti-CrATG4 (1:250) and antiacetylated Tubulin (Sigma-Aldrich; T7451; 1:500 dilution). For signal detection, fluorescein isothiocyanate-labeled goat anti-rabbit antibody (Sigma-Aldrich; F4890; 1:500 dilution) and Alexa Fluor 594 donkey anti-mouse (Jackson ImmunoResearch; 715-515-150; 1:5,000 dilution) were used. Preparations were photographed on a DM6000B microscope (Leica) with an ORCA-ER camera (Hamamatsu) and processed with the Leica Application Suite Advanced Fluorescence software package (Leica). For comparative analysis, the same acquisition time was fixed for the fluorescein isothiocyanate or Alexa Fluor 594 signals.

Statistical Methods

All experiments were performed at least in triplicate and data are presented as mean \pm SD. The statistical significance of data was verified by the Student's *t* test whenever required.

Supplemental Data

The following supplemental materials are available.

Supplemental Figure S1. Table showing the identity (%) of ATG4 proteins from different species.

Supplemental Figure S2. Unrooted maximum likelihood phylogenetic tree of ATG4 proteins.

Supplemental Figure S3. Multiple sequence alignment of ATG4 from diverse organisms.

Supplemental Figure S4. Redox control of yeast ATG4 oligomerization.

Supplemental Figure S5. Detection of ATG4 in total extracts from *C. reinhardtii*.

Supplemental Table S1. Proteins used in this study.

ACKNOWLEDGMENTS

We thank Christophe Marchand for sharing *C. reinhardtii* TRXh1 and TRXh1C39S proteins, Emmanuelle Issakidis-Bourguet for kindly providing Arabidopsis NTRB, Krishna Niyogi for making carotenoid mutant strains available to the research community, and Francisco J. Florencio for critical reading of the manuscript.

Received October 12, 2016; accepted October 15, 2016; published October 17, 2016.

LITERATURE CITED

- Avila-Ospina L, Moison M, Yoshimoto K, Masclaux-Daubresse C (2014) Autophagy, plant senescence, and nutrient recycling. *J Exp Bot* **65**: 3799–3811
- Avin-Wittenberg T, Honig A, Galili G (2012) Variations on a theme: plant autophagy in comparison to yeast and mammals. *Protoplasma* **249**: 285–299
- Bassham DC, Laporte M, Marty F, Moriyasu Y, Ohsumi Y, Olsen LJ, Yoshimoto K (2006) Autophagy in development and stress responses of plants. *Autophagy* **2**: 2–11
- Buchanan BB, Balmer Y (2005) Redox regulation: a broadening horizon. *Annu Rev Plant Biol* **56**: 187–220
- Chung T, Suttangkakul A, Vierstra RD (2009) The ATG autophagic conjugation system in maize: ATG transcripts and abundance of the ATG8-lipid adduct are regulated by development and nutrient availability. *Plant Physiol* **149**: 220–234
- Crespo JL, Díaz-Troya S, Florencio FJ (2005) Inhibition of target of rapamycin signaling by rapamycin in the unicellular green alga *Chlamydomonas reinhardtii*. *Plant Physiol* **139**: 1736–1749
- Davey MP, Horst I, Duong GH, Tomsett EV, Litvinenko AC, Howe CJ, Smith AG (2014) Triacylglyceride production and autophagous responses in *Chlamydomonas reinhardtii* depend on resource allocation and carbon source. *Eukaryot Cell* **13**: 392–400
- Dengjel J, Hoyer-Hansen M, Nielsen MO, Eisenberg T, Harder LM, Schandorff S, Farkas T, Kirkegaard T, Becker AC, Schroeder S, et al (2012). Identification of autophagosome-associated proteins and regulators by quantitative proteomic analysis and genetic screens. *Mol Cell Proteomics* **11**: M111.014035
- Díaz-Troya S, Florencio FJ, Crespo JL (2008a) Target of rapamycin and LST8 proteins associate with membranes from the endoplasmic reticulum in the unicellular green alga *Chlamydomonas reinhardtii*. *Eukaryot Cell* **7**: 212–222
- Díaz-Troya S, Pérez-Pérez ME, Florencio FJ, Crespo JL (2008b) The role of TOR in autophagy regulation from yeast to plants and mammals. *Autophagy* **4**: 851–865
- Dietz KJ (2011) Peroxiredoxins in plants and cyanobacteria. *Antioxid Redox Signal* **15**: 1129–1159
- Farmer LM, Rinaldi MA, Young PG, Danan CH, Burkhart SE, Bartel B (2013) Disrupting autophagy restores peroxisome function to an Arabidopsis lon2 mutant and reveals a role for the LON2 protease in peroxisomal matrix protein degradation. *Plant Cell* **25**: 4085–4100
- Feng Y, He D, Yao Z, Klionsky DJ (2014) The machinery of macroautophagy. *Cell Res* **24**: 24–41
- Floyd BE, Morriss SC, Macintosh GC, Bassham DC (2012) What to eat: evidence for selective autophagy in plants. *J Integr Plant Biol* **54**: 907–920
- Goodenough U, Blaby I, Casero D, Gallaher SD, Goodson C, Johnson S, Lee JH, Merchant SS, Pellegrini M, Roth R, et al (2014) The path to triacylglyceride obesity in the sta6 strain of *Chlamydomonas reinhardtii*. *Eukaryot Cell* **13**: 591–613
- Goyer A, Decottignies P, Lemaire S, Ruelland E, Issakidis-Bourguet E, Jacquot JP, Miginiac-Maslow M (1999) The internal Cys-207 of sorghum leaf NADP-malate dehydrogenase can form mixed disulphides with thioredoxin. *FEBS Lett* **444**: 165–169
- Harris EH (1989) The Chlamydomonas Sourcebook. Academic Press, San Diego
- He C, Klionsky DJ (2009) Regulation mechanisms and signaling pathways of autophagy. *Annu Rev Genet* **43**: 67–93
- Ishida H, Yoshimoto K, Izumi M, Reisen D, Yano Y, Makino A, Ohsumi Y, Hanson MR, Mae T (2008) Mobilization of rubisco and stroma-localized fluorescent proteins of chloroplasts to the vacuole by an ATG gene-dependent autophagic process. *Plant Physiol* **148**: 142–155
- Jacquot JP, Rivera-Madrid R, Marinho P, Kollarova M, Le Maréchal P, Miginiac-Maslow M, Meyer Y (1994) Arabidopsis thaliana NAPHP thioredoxin reductase. cDNA characterization and expression of the recombinant protein in *Escherichia coli*. *J Mol Biol* **235**: 1357–1363
- Kim J, Lee H, Lee HN, Kim SH, Shin KD, Chung T (2013) Autophagy-related proteins are required for degradation of peroxisomes in Arabidopsis hypocotyls during seedling growth. *Plant Cell* **25**: 4956–4966
- Kirisako T, Ichimura Y, Okada H, Kabeya Y, Mizushima N, Yoshimori T, Ohsumi M, Takao T, Noda T, Ohsumi Y (2000) The reversible modification regulates the membrane-binding state of Apg8/Aut7 essential for autophagy and the cytoplasm to vacuole targeting pathway. *J Cell Biol* **151**: 263–276
- Kong-Hap MA, Mouammine A, Daher W, Berry L, Lebrun M, Dubremetz JF, Besteiro S (2013) Regulation of ATG8 membrane association by ATG4 in the parasitic protist *Toxoplasma gondii*. *Autophagy* **9**: 1334–1348
- Lemaire SD, Miginiac-Maslow M (2004) The thioredoxin superfamily in *Chlamydomonas reinhardtii*. *Photosynth Res* **82**: 203–220
- Li F, Vierstra RD (2012) Autophagy: a multifaceted intracellular system for bulk and selective recycling. *Trends Plant Sci* **17**: 526–537
- Liu Y, Bassham DC (2012) Autophagy: pathways for self-eating in plant cells. *Annu Rev Plant Biol* **63**: 215–237
- McCarthy SS, Kobayashi MC, Niyogi KK (2004) White mutants of *Chlamydomonas reinhardtii* are defective in phytoene synthase. *Genetics* **168**: 1249–1257
- Michaeli S, Galili G, Genschik P, Fernie AR, Avin-Wittenberg T (2016) Autophagy in plants—What's new on the menu? *Trends Plant Sci* **21**: 134–144
- Minina EA, Bozhkov PV, Hofius D (2014) Autophagy as initiator or executioner of cell death. *Trends Plant Sci* **19**: 692–697
- Mizushima N, Yoshimori T, Ohsumi Y (2011) The role of Atg proteins in autophagosome formation. *Annu Rev Cell Dev Biol* **27**: 107–132
- Nair U, Yen WL, Mari M, Cao Y, Xie Z, Baba M, Reggiori F, Klionsky DJ (2012) A role for Atg8-PE deconjugation in autophagosome biogenesis. *Autophagy* **8**: 780–793
- Nakatogawa H, Ishii J, Asai E, Ohsumi Y (2012) Atg4 recycles inappropriately lipidated Atg8 to promote autophagosome biogenesis. *Autophagy* **8**: 177–186
- Oku M, Sakai Y (2016) Pexophagy in yeasts. *Biochim Biophys Acta* **1863**: 992–998
- Pérez-Martín M, Blaby-Haas CE, Pérez-Pérez ME, Andrés-Garrido A, Blaby IK, Merchant SS, Crespo JL (2015) Activation of autophagy by metals in *Chlamydomonas reinhardtii*. *Eukaryot Cell* **14**: 964–973
- Pérez-Martín M, Pérez-Pérez ME, Lemaire SD, Crespo JL (2014) Oxidative stress contributes to autophagy induction in response to endoplasmic reticulum stress in *Chlamydomonas reinhardtii*. *Plant Physiol* **166**: 997–1008
- Pérez-Pérez ME, Florencio FJ, Crespo JL (2010) Inhibition of target of rapamycin signaling and stress activate autophagy in *Chlamydomonas reinhardtii*. *Plant Physiol* **152**: 1874–1888
- Pérez-Pérez ME, Couso I, Crespo JL (2012) Carotenoid deficiency triggers autophagy in the model green alga *Chlamydomonas reinhardtii*. *Autophagy* **8**: 376–388
- Pérez-Pérez ME, Crespo JL (2014) Autophagy in algae. *Perspect Phycol* **1**: 93–102
- Pérez-Pérez ME, Zaffagnini M, Marchand CH, Crespo JL, Lemaire SD (2014) The yeast autophagy protease Atg4 is regulated by thioredoxin. *Autophagy* **10**: 1953–1964
- Sandmann G, Albrecht M (1990) Accumulation of colorless carotenes and derivatives during interaction of bleaching herbicides with phytoene desaturation. *Z Naturforsch C* **45**: 487–491
- Schatz D, Shemi A, Rosenwasser S, Sabanay H, Wolf SG, Ben-Dor S, Vardi A (2014) Hijacking of an autophagy-like process is critical for the life cycle of a DNA virus infecting oceanic algal blooms. *New Phytol* **204**: 854–863
- Scherz-Shouval R, Shvets E, Fass E, Shorer H, Gil L, Elazar Z (2007) Reactive oxygen species are essential for autophagy and specifically regulate the activity of Atg4. *EMBO J* **26**: 1749–1760

- Schreiber A, Peter M** (2014) Substrate recognition in selective autophagy and the ubiquitin-proteasome system. *Biochim Biophys Acta* **1843**: 163–181
- Shemi A, Ben-Dor S, Vardi A** (2015) Elucidating the composition and conservation of the autophagy pathway in photosynthetic eukaryotes. *Autophagy* **11**: 701–715
- Shibata M, Oikawa K, Yoshimoto K, Kondo M, Mano S, Yamada K, Hayashi M, Sakamoto W, Ohsumi Y, Nishimura M** (2013) Highly oxidized peroxisomes are selectively degraded via autophagy in Arabidopsis. *Plant Cell* **25**: 4967–4983
- Sugawara K, Suzuki NN, Fujioka Y, Mizushima N, Ohsumi Y, Inagaki F** (2005) Structural basis for the specificity and catalysis of human Atg4B responsible for mammalian autophagy. *J Biol Chem* **280**: 40058–40065
- Tsukada M, Ohsumi Y** (1993) Isolation and characterization of autophagy-defective mutants of *Saccharomyces cerevisiae*. *FEBS Lett* **333**: 169–174
- Woo J, Park E, Dinesh-Kumar SP** (2014) Differential processing of Arabidopsis ubiquitin-like Atg8 autophagy proteins by Atg4 cysteine proteases. *Proc Natl Acad Sci USA* **111**: 863–868
- Xiong Y, Contento AL, Nguyen PQ, Bassham DC** (2007) Degradation of oxidized proteins by autophagy during oxidative stress in Arabidopsis. *Plant Physiol* **143**: 291–299
- Yoshimoto K, Hanaoka H, Sato S, Kato T, Tabata S, Noda T, Ohsumi Y** (2004) Processing of ATG8s, ubiquitin-like proteins, and their deconjugation by ATG4s are essential for plant autophagy. *Plant Cell* **16**: 2967–2983
- Young PG, Bartel B** (2016) Pexophagy and peroxisomal protein turnover in plants. *Biochim Biophys Acta* **1863**: 999–1005
- Yu ZQ, Ni T, Hong B, Wang HY, Jiang FJ, Zou S, Chen Y, Zheng XL, Klionsky DJ, Liang Y, et al** (2012) Dual roles of Atg8-PE deconjugation by Atg4 in autophagy. *Autophagy* **8**: 883–892

Figure S1. Table showing the identity (%) of ATG4 proteins from different species (*Chlamydomonas reinhardtii*; *Volvox carteri*; *Coccomyxa subellipsoidea*; *Arabidopsis thaliana*; *Oryza sativa*; *Homo sapiens*; *Saccharomyces cerevisiae*; *Schizosaccharomyces pombe*). The identity was obtained by alignment of the two sequences using Pairwise Sequence Alignment EMBOSS Needle. The accession numbers are indicated in Figure S2.

Figure S2. Unrooted Maximum likelihood phylogenetic tree of ATG4 proteins. Sub-families are indicated by color-coded circles. Species abbreviations and the accession numbers are indicated. **Cr:** *Chlamydomonas reinhardtii* (Cre12.g510100.t1.1), **Vc:** *Volvox carteri* (Vocar.0016s0213.1), **Cs:** *Coccomyxa subellipsoidea* (EIE27123), **At:** *Arabidopsis thaliana* (AT2G44140.1 for A; AT3G59950.1 for B), **Al:** *Arabidopsis lyrata* (935334 for A; 486460 for B), **Zm:** *Zea mays* (GRMZM2G064212_T02 for A; GRMZM2G173682_T01 for B), **Sl:** *Solanum lycopersicum* (Solyc01g006230.2.1), **St:** *Solanum tuberosum* (PGSC0003DMT400081879), **Gm:** *Glycine max* (Glyma.18G248400.1 for A; Glyma.09G244800.1 for B), **Mt:** *Medicago truncatula* (Medtr7g081230.1), **Vv:** *Vitis vinifera* (GSVIVT01003913001), **Os:** *Oryza sativa* (LOC_Os03g27350.1 for A; LOC_Os04g58560.1 for B), **Sc:** *Saccharomyces cerevisiae* (KZV08400), **Sp:** *Schizosaccharomyces pombe* (CAC00556), **Ca:** *Candida albicans* (XP_713234), **Nc:** *Neurospora crassa* (EAA30202), **An:** *Aspergillus nidulans* (XP_661074), **Hs:** *Homo sapiens* (BAB83889 for A; BAB83890 for B), **Mm:** *Mus musculus* (NP_777364 for A; NP_777363 for B), **Zf:** *Zebrafish* (AAH95617), **Dm:** *Drosophila melanogaster* (NP_608563). ATG4 sequences were obtained from Phytozome (<https://phytozome.jgi.doe.gov/pz/portal.html>) for algae and plants, and NCBI (<https://www.ncbi.nlm.nih.gov/pubmed>) for fungi and animals.

Figure S3. Multiple sequence alignment of ATG4 from diverse organisms. (A) Alignment of the region containing the catalytic Cys84. **(B)** Alignment of the C-terminus region containing putative regulatory Cys400 and Cys473. The proteins were aligned with the ClustalW program using default parameters. Residues boxed in red correspond to 70% identity. Residues boxed in blue correspond to 70% conservation with the PAM120 matrix. The accession numbers are indicated in Figure S2.

Figure S4. Redox control of yeast ATG4 oligomerization. (A) Yeast recombinant ATG4 (5 μ M) was subjected to 12 % SDS-PAGE in the presence (+) or absence (-) of β -mercaptoethanol (β ME) and stained with coomassie brilliant blue (CBB). mATG4, monomeric ATG4; oATG4, oligomeric ATG4. (B) ATG4 (5 μ M) was preincubated with 100 μ M DTT for 1 h (lane 2); then, ATG4 was treated with 500 μ M H₂O₂ for 20 min (lane 3); and finally, ATG4 was incubated with 1 mM DTT for 30 min (lane 4). Control (lane 1): incubation with no addition. (C) Redox titration of ATG4 oligomerization/monomerization. ATG4 monomerization was analyzed after incubation for 2 h at indicated E_h poised by 20 mM DTT in various dithiol/disulfide ratios. Arrowheads indicate oligomeric (oATG4) and monomeric (mATG4) ATG4 forms. β -mercaptoethanol-free buffer was used in (B and C).

Figure S5. Detection of ATG4 in total extracts from Chlamydomonas. Different amounts (2.5, 10, 20, 30 and 40 μ g) of soluble extracts from stationary cells were resolved by 12 % SDS-PAGE followed by Western-blot analysis with the anti-ATG4 antibody. The oligomeric (oATG4) and monomeric (mATG4) ATG4 forms are marked on the right. Molecular mass markers (kDa) are indicated on the left. β -mercaptoethanol-free buffer was used.

Figure Suppl 2

green lineage

higher plants

algae

metazoa

fungi

0.2

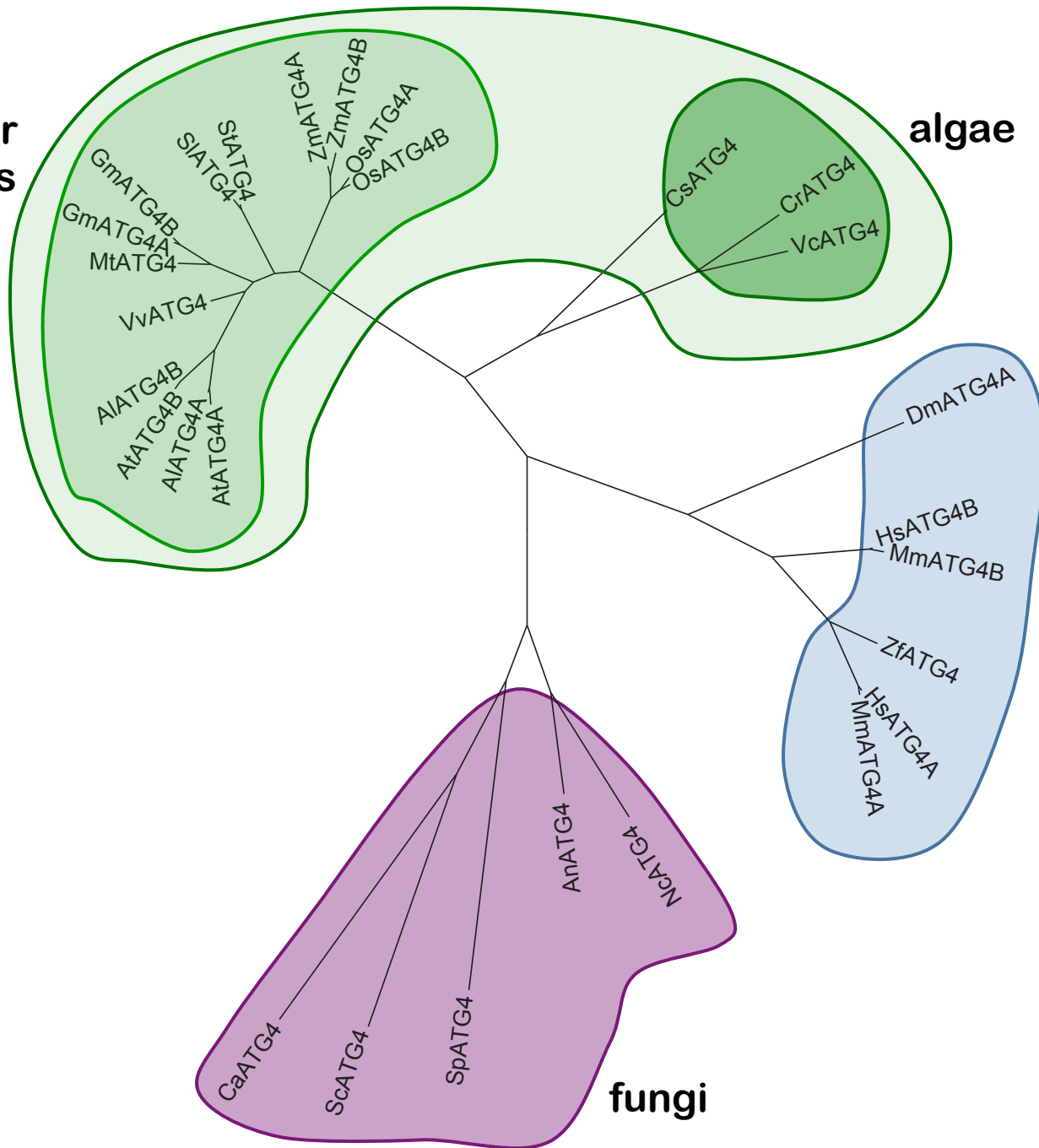


Figure Suppl 4

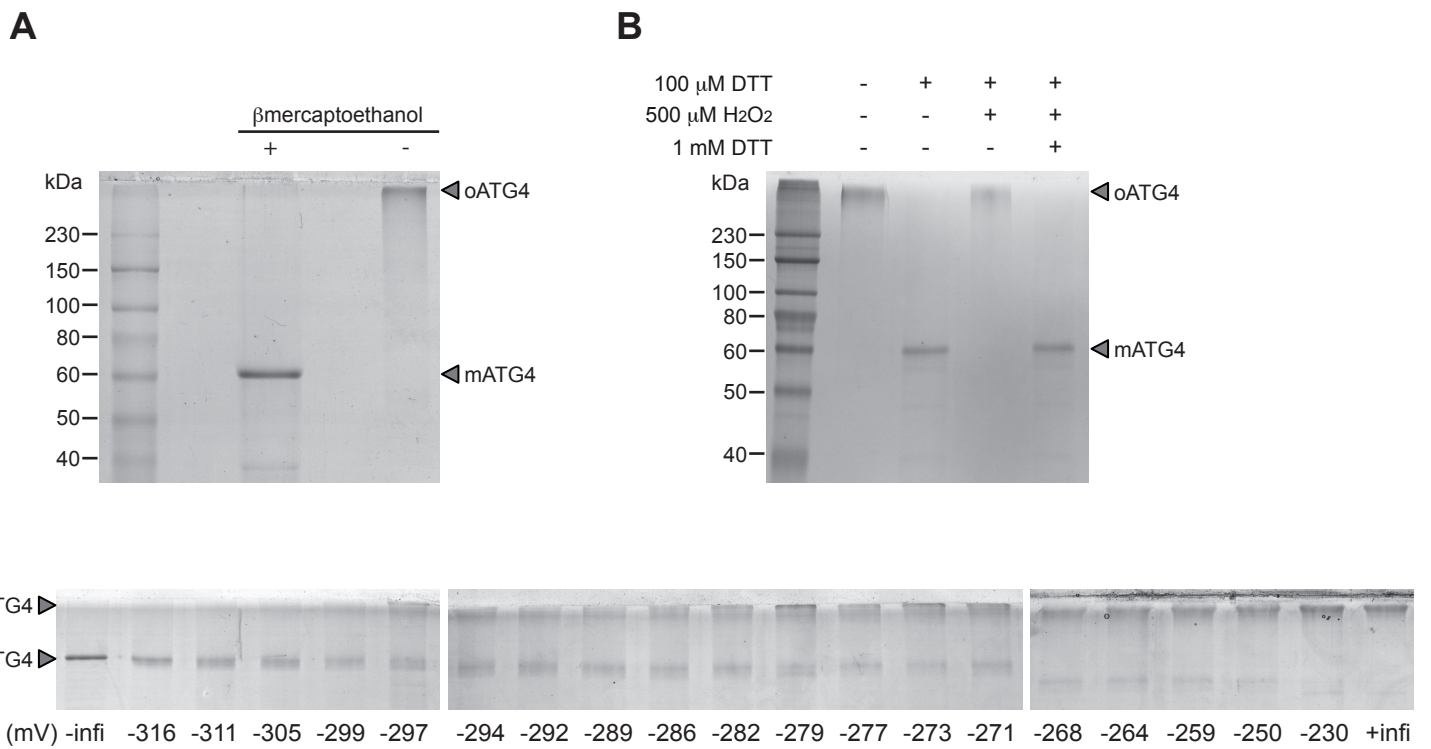


Figure Suppl 5

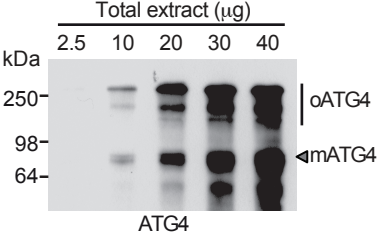


Table S1. Proteins used in this study

Name	Characteristics	Reference
CrATG8^{WT}	His-tag CrATG8	1
CrATG4^{WT}	His-tag CrATG4	This study
CrATG4^{C84S}	His-tag CrATG4 where Cys84 was replaced by Ser	This study
CrATG4^{C400S}	His-tag CrATG4 where Cys400 was replaced by Ser	This study
CrATG4^{C473S}	His-tag CrATG4 where Cys473 was replaced by Ser	This study
ScATG4^{WT}	His-tag ScATG4	2
CrTRXh1	His-tag ScTrx1	3
CrTRXh1^{C39S}	His-tag ScTrx1 where Cys33 was replaced by Ser	3
AtNTRB	His-tag AtNTRB	4

Cr: *Chlamydomonas reinhardtii*; **Sc:** *Saccharomyces cerevisiae*; **At:** *Arabidopsis thaliana*.

1. Pérez-Pérez ME, Florencio FJ, Crespo JL (2010). *Plant Physiol*, 152:1874-1888.
2. Pérez-Pérez ME, Zaffagnini M, Marchand CH, Crespo JL, Lemaire SD (2014). *Autophagy*, 10(11):1953-1964.
3. Goyer A, Decottignies P, Lemaire S, Ruelland E, Issakidis-Bourguet E, Jacquot J-P, Miginiac-Maslow M (1999). *FEBS Lett*, 444(2-3):165-169.
4. Jacquot J-P, Rivera-Madrid R, Marinho P, Kollarova M, Le Maréchal P, Miginiac-Maslow M, Meyer Y (1994). *J. Mol. Biol.*, 235(4):1357-1363.